Drought dynamics explain once in a century yellow fever virus outbreak in Brazil with implications for climate change

Jamie M. Caldwell[1*], Bryan Grenfell[1,2], Gabriel Vecchi[1,3], Joelle I. Rosser[4*]

[1*]High Meadows Environmental Institute, Princeton University, Guyot Hall, Princeton, 08544, New Jersey, USA.
[2]Department of Ecology and Evolutionary Biology, Princeton University, Guyot Hall, Princeton, 08544, New Jersey, USA.
[3]Department of Geosciences, Princeton University, Guyot Hall, Princeton, 08544, New Jersey, USA.
[4*]Stanford University School of Medicine, Stanford University, 291 Campus Drive, Stanford, 94305, California, USA.

*Corresponding author(s). E-mail(s): jamie.caldwell@princeton.edu; jrosser@stanford.edu;
Contributing authors: grenfell@princeton.edu; gvecchi@princeton.edu;

Abstract

While excess rainfall is associated with mosquito-borne disease because it supports mosquito breeding, drought may also counterintuitively increase disease transmission by altering mosquito and host behavior. This phenomenon is important to understand because climate change is projected to increase both extreme rainfall and drought. In this study, we investigated the extent to which seasonally-driven mosquito and primate behavior drove the first urban yellow fever virus (YFV) epidemic in Brazil in a century, coinciding with an equally rare drought, and to assess the role of interventions in ending the outbreak. We hypothesized that drought triggered the outbreak by driving the forest mosquitoes and non-human primates towards the city in search of water and that the mosquitoes were biting more frequently to avoid desiccation. A dynamical YFV model supports these hypotheses, showing that increased mosquito biting can explain the second peak in transmission while primate movement determined the timing and magnitude of transmission. Further, a combination of vector control, vaccination, and

conservation measures likely contributed to ending the outbreak. Together, these results suggest that drought—likely to become more frequent in this region in the coming decades—can significantly influence mosquito-borne disease transmission, and that sustained control will require multiple interventions.

Keywords: arbovirus, non-human primates, extreme weather events, global change

1 Introduction

After nearly a century without urban yellow fever virus (YFV) transmission, Brazil experienced a major outbreak in 2017-18 ([1, 2]), likely driven by a combination of land use change, viral evolution, accumulation of susceptible populations, and favorable climate conditions. YFV causes disease in humans and non-human primates with clinical presentations ranging from asymptomatic to life-threatening. YFV spreads via an urban transmission cycle involving *Aedes aegypti* mosquitoes and humans, or a sylvatic (i.e., forest) cycle between forest mosquitoes, non-human primates, and occasionally humans. While aggressive vector control and vaccination had controlled the urban cycle ([3, 4]), intensive land use change facilitated spillover from the sylvatic cycle into rural human populations at the forest edge ([5]). As deforestation increased, YFV spread southeastward in Brazil leading up to the 2017-18 outbreak, which was first reported in Minas Gerais and then in neighboring states of Espiritu Santo, Rio, and Sao Paulo ([1, 6]). The virus may have evolved increased transmutability during this time through phenotypic changes in nonstructural proteins ([7]), and historically low vaccination rates due to low YFV risk ([8]) left a large pool of susceptible individuals despite the high efficacy of the vaccine ([9]). Together, these factors suggest that sylvatic mosquito vectors were carrying more transmissible strains of the virus and living in closer proximity to dense human populations with limited vaccine coverage ([8]). Against this backdrop, an extreme drought ([6, 10]) may have triggered the outbreak by increasing contact between infected mosquitoes and humans, consistent with models identifying low vaccine coverage, high population density, and climate factors as key drivers of YFV spillover risk ([11]).

Given the role of water in the mosquito life cycle, there is an intuitive reason to suspect excess precipitation to increase YFV incidence, however, drought could also influence disease dynamics by concentrating hosts and vectors in the same locations and times and/or by increasing mosquito feeding to counteract dehydration. Drought is not normally considered a major driver of YFV in part because most urban epidemics are seeded by an importation event (e.g., a traveler) or through the bite of a forest or bridge vector, but then transmission is sustained in the human population by the urban mosquito, *Aedes aegypti*. In this outbreak however, there are multiple lines of evidence that suggest forest mosquitoes, primarily in the genus *Haemogogus*, were responsible for sustained human transmission ([1, 12–15]). A *Haemogogus*-driven outbreak implies the presence of forest mosquitoes in the city and regular contact with people. While *Haemogogus* will bite people, they more commonly bite non-human primates (e.g., howler monkeys and marmosets). This feeding behavior could still have

played a critical role in the urban outbreak as non-human primate carcasses were found in and around the city. Even though there were likely fewer non-human primates than humans in the cities, they could have disproportionately contributed to transmission because non-human primates are highly susceptible to and infectious carriers of YFV ([12–14, 16, 17]). Large scale presence of *Haemogogus* and non-human primates in the city is unusual, but plausible given the climatic conditions. The YFV epidemic had two peaks in incidence occurring around the height of the rainy season in 2017 and 2018; during the extreme drought ([6, 10]), the modest rainfall during those periods could explain both increased feeding and contact because when water is scarce, mosquitoes and non-human primates will move farther to find water and mosquitoes will bite more often to avoid desiccation.

To evaluate the extent to which seasonally-driven mosquito feeding and non-human primates incursion into the cities could have contributed to the 2017-18 outbreak and assess intervention strategies, we simulated YFV transmission with a compartmental model parameterized based on different hypotheses and compared those outputs with real world evidence. We developed a compartmental model that captures key features of the Brazil YFV epidemic, including transmission from *Haemogogus* and *Aedes aegypti* mosquitoes to non-human primates (howler monkeys and marmosets) and humans (Figure 1). The model accounts for differential mosquito feeding preferences, reduced *Aedes aegypti* abundance due to prior vector control, and the movement of howler monkeys into urban areas during the outbreak. Within this model structure, we asked how well the model reproduced disease dynamics in Minas Gerais during the epidemic with nested models accounting for seasonally-driven mosquito feeding behavior, howler monkey movement, or both. Then we assessed the extent to which different interventions could have reduced the second wave of transmission and if those interventions would carry into the future.

2 Results

2.1 Comparison of seasonal drivers

The model that incorporated both seasonally-driven primate movement and mosquito biting behavior (hereafter referred to as the *base model*) reproduced the observed two-year epidemic dynamics in both humans and NHP better than the nested versions of this model (Figure 2, Table 1). The base model captured the epidemic seasonality well and a sensitivity analysis supports the robustness of these conclusions (Table A1). The nested model that incorporated seasonally-driven mosquito biting but restricted primate movement reproduced a two-peak epidemic but predicted a late peak in cases and fewer cases overall compared with the observations. In contrast, the model that incorporated seasonally-driven primate movement but restricted seasonally-driven mosquito biting reproduced the first wave of the epidemic well but did not generate a second wave of transmission as was observed. The model that restricted both seasonally-driven mosquito biting and primate movement poorly predicted both waves of transmission: the model inaccurately predicted the timing and incidence for the first peak and did not predict a second peak. Together, these results indicate that increased mosquito biting during the rainy season, partially driven by

the ongoing drought conditions, was responsible for the occurrence of the second peak in transmission, while primate movement was responsible for the timing and magnitude of the second peak, given the mosquitoes were present and biting. All models predicted the initial wave of transmission well.

Table 1 Correlation (p-value) between model predictions and observations across nested seasonally-driven models. Modeled human cases were adjusted by a one month lead time. Note that the 'No seasonality' model still includes a seasonal mosquito carrying capacity.

Model	Human cases	NHP cases	Average correlation
Base model	0.74 ($p < 0.001$)	0.93 ($p < 0.001$)	0.84
Seasonally-driven primate movement only	0.23 ($p > 0.05$)	0.42 ($p < 0.05$)	0.33
Seasonally-driven mosquito biting only	0.54 ($p < 0.01$)	0.67 ($p < 0.001$)	0.61
No seasonality	0.07 ($p > 0.05$)	0.25 ($p > 0.05$)	0.16

2.2 Optimizing Interventions

To reduce both short- and long-term YFV outbreaks in this system, we found that multiple interventions must be employed simultaneously (Figure 3). The intervention that reflected spraying insecticides every rainy season, the key vector control tactic used in the region, led to a small reduction in cases in the short term but allowed for increasingly large annual outbreaks due to the buildup of mosquito populations. The intervention that reflected conservation initiatives aimed at reducing movement of primates from the forest to the city reduced short-term transmission substantially, but those impacts lessened over time allowing annual outbreaks to grow slightly bigger each year after the initial honeymoon phase. The third intervention initiated the vaccination campaign at the onset of the epidemic (whereas in reality the campaign was delayed until after the first peak) and then continued YFV vaccination as part of routine childhood vaccinations in the region; this intervention did not affect the first or second waves strongly but continued to decrease cases annually, contrasting the patterns of the first two interventions described. Only the simulation that included all three interventions showed substantial and sustained control of YFV. If the virus evolved to be 50% more transmissible, which would be possible in the future, even stronger integrated control would be needed.

2.3 Extreme drought and global change

The drought prior to the 2017-18 YFV outbreak in Minas Gerais, Brazil was 9.5% more extreme than a once in a century drought (i.e., 100-yr return period) and dry conditions are projected to increase in the future (Figure 4). Based on the widely used drought metric, Standardized Precipitation Evapotranspiration Index (SPEI), we show that extreme dry conditions were present four months prior to the YFV outbreak. This timeline aligns with the expected bio-physical process that links climate to disease transmission whereby dry conditions promote migration of non-human primates and forest mosquitoes towards city centers in search of food and water in the months

preceding the outbreak. Based on climate models, future conditions in this region are 47% drier than historical conditions at the 1% exceedance threshold, indicating a substantial increase in the severity of extreme drought events (based on projections with intermediate greenhouse gas emissions: SSP245). The IPCC-AR6 supports that drought should increase in Brazil (Figure 12.4 from [18]).

3 Discussion

Yellow fever virus (YFV) outbreaks are notoriously difficult to predict, and retrospective analyses can provide some insight into why outbreaks begin and why they end. The 2017-18 outbreak in southeastern Brazil was particularly unusual because there had not been urban transmission in the region in nearly a century. Prior studies hypothesized that slow changes (e.g., build up of a highly susceptible population, land use change) provided the background conditions for an outbreak to emerge ([11]), while we tested the hypothesis that seasonal climate conditions triggered the outbreak ([6]). By comparing models representing different hypotheses about seasonal drivers with real world observations, we show that seasonally-driven mosquito feeding behavior likely explains the magnitude of transmission, while seasonally-driven non-human primates incursion into the city explains the outbreak timing, especially with respect to the second wave of transmission. Even without drought conditions however, it is possible that once seeded, an outbreak would have taken off, simply do to high susceptibility in the population. While seasonal climate appears to explain how the outbreak developed, it is equally important to understand why the outbreak did not continue to cause annual epidemics thereafter. The intervention simulations show that a combination of activities likely contained the outbreak. In reality, the three techniques described (vector control, vaccination, conservation) were employed to different extents and largely align with real-life observations, where YFV cases were not reported after 2018. The simulations suggest that if the interventions were deployed earlier, the second wave of transmission may have been avoided, although the model does not account for real and important logistical difficulties that likely delayed the interventions. The simulations also suggest that there could be very low levels of continued transmission. Given the high rate of asymptomatic transmission ([19]), it is plausible that some cases go undetected every year.

The Brazilian epidemic was also unusual because it spread in urban areas but was predominantly spread by a non-urban mosquito species, amplified by non-human primate transmission. The outbreak was driven by *Haemogogus* rather than *Aedes aegypti* mosquitoes. The expectation was that given sufficient cases, there would be re-establishment of an urban transmission cycle perpetuated by *Aedes aegypti*–human transmission as *Aedes aegypti* remains a competent YFV vector in laboratory studies ([20, 21]). However, no infected *Aedes aegypti* were found during this outbreak ([22, 23, 23–25]). Thus, this outbreak was largely driven by *Haemogogus* flexibly feeding on alternate hosts, which has been reported previously ([26–28]), and was likely bolstered by feeding on non-human primates in the city, which have higher and longer viremia profiles than people ([1, 2]), indicating even low abundances of non-human primates can impact transmission. The contribution of non-human primates in urban

transmission may also be the reason vaccination alone did not appear adequate to reduce transmission in the short term. Our expectation was that to limit outbreaks (i.e., R_0 <1), vaccination coverage needed to be 76-79% (coverage required to limit outbreaks = 1 - $1/R_0$ where median $R_0 = 4.21$, mean $R_0 = 4.81$; [29]). In this study, we allowed vaccination coverage to reach 90%, yet the simulations showed vaccination alone could not have prevented the second wave of transmission, suggesting we should consider the susceptible population as a combination of people and non-human primates. A related important consideration is that continued viral evolution will increase the critical population size necessary for disease control. Thus, a suite of integrated control measures will become increasingly important.

Land use change was likely the proximate cause of non-human primate incursion into the city and ecological countermeasures may be key to reducing future disease emergence risk. Deforestation and other types of habitat alteration can increase spillover risk of disease from the forest to the city by affecting non-human primate susceptibility and spatial behavior ([30]). Reduced habitat quality and area often limit food and water availability, forcing non-human primates to invest extra physiological resources for basic survival, leading to reduced immune function. Immune dysregulation can both increase susceptibility to infection and increase pathogen loads and shedding time ([30]). Additionally, animals may need to expand their search area to find food ([30–33]). These behavioral changes then increase the likelihood and length of infected non-human primates- *Haemogogus* contact within cities where *Haemogogus* are also biting people. Ecological countermeasures, or conservation initiatives, are therefore an effective strategy for primary protection against spillover events; such measures include protecting and restoring wildlife habitat, creating buffer zones, and strategically safeguarding critical habitat for animal feeding, resting, and social aggregation, ultimately strengthening barriers that separate (infected) wildlife and vectors from people ([30]).

Another pillar of epidemic prevention is vaccination. The YFV vaccine is highly efficacious, well studied, and largely available to high risk populations ([9]). Since southeastern Brazil had not experienced a YFV outbreak in nearly a century, most of the region was not considered high risk and was under-vaccinated at the start of the epidemic ([8]). Perhaps more problematic than under-vaccination though, was that in parts of Minas Gerais where YFV vaccinations programs were in place prior to the 2017-18 outbreak, coverage was incomplete and levels of neutralizing antibodies were undetectable across a large proportion of the population ([34, 35]), including in individuals with a documented history of YFV vaccination ([35]). Undetectable levels of neutralizing antibodies indicate waning immunity, which is surprising given the WHO has deemed a single dose of the YFV vaccine confers lifelong immunity, but plausible given some other studies ([36]). This is an important finding as vaccines that do not confer lifelong immunity require different vaccine schedules than those that do and have different implications for long term disease dynamics. Additional issues that should be considered in epidemic prevention planning are potential bottlenecks such as vaccine shortages, cold transport delays, or distribution problems.

4 Conclusion

The central premise of this study was to investigate the role that drought may have played in triggering an outbreak, building on a growing body of evidence linking the two, to ultimately understand how climate and climate change affect infectious disease dynamics. Among the different climate-change related hazards that can affect climate-sensitive infectious diseases, drought is a relatively difficult one to examine. Unlike heatwaves or floods, which are usually distinct events, drought conditions build slowly and can last months to years or more. As a result, robustly linking drought to an epidemic is difficult because of the differing time scales. Despite this challenge, a handful of studies have examined the relationship between drought and a variety of water-borne and vector-borne diseases and consistently found a positive relationship between them. In this study we provide support for two mechanisms for this relationship: 1) drought can cause non-human primate hosts and competent mosquito vectors to move towards human inhabited spaces, and 2) mosquito vectors bite more frequently to avoid desiccation, leading to more opportunities for transmission. Climate change allows droughts to set in quicker and become more intense, so we would expect drought-disease dynamics to become more prominent, yet there are many challenges in developing reliable drought assessments under climate change, making our ability to anticipate such events nontrivial ([37]). On the other hand, the slow build up of drought relative to other events with short lead times like cyclones and floods, provides an opportunity for anticipatory action from health systems as soon as drought conditions start to build. This knowledge could therefore be used to develop early warning systems to better support decision makers and health system planning, both for YFV and potentially other arboviruses.

5 Methods

5.1 Model and Parameters

We developed a compartmental model to simulate transmission dynamics for yellow fever virus in Brazil, accounting for key features of the dynamical system. It includes both *Haemogogus* and *Aedes aegypti* mosquitoes as vectors and howler monkeys (genus *Aloutta*), marmosets (genus *Calithrix*), and humans as hosts (Figure 1). Within each species, individuals move between some combination of susceptible, exposed, infectious, and removed (i.e., recovered/dead) states (Figure 1). To account for differential feeding preferences, *Haemogogus* mosquitoes bite non-human primate hosts more often than people while *Aedes aegypti* exclusively bite people. This acknowledges that *Haemogogus* mosquitoes typically bite non-human primates in the canopy, only descending and moving to bite people when the forest environment is disturbed or canopy hosts are scarce ([27, 28]). The abundance of *Aedes aegypti* in the model also reflects population estimates at the time of the epidemic, which were approximately 2-3 times lower than in the previous decade due to extensive vector control efforts in response to the Zika pandemic (based on a Rapid Index Survey for Aedes aegypti by the Prefeitura Do Rio de Janeiro). Additionally, the model allows howler monkeys to move into the city as they are highly adapted to fragmented peri-urban habitats

([12, 13, 17, 38]) and many more carcasses were found in and around the city than a typical year ([6]). We describe the set of ordinary differential equations that describe the model below with associated parameter definitions and values in Table 2.

Howler monkeys

$$\frac{dS_p}{dt} = -\alpha_1[t] \cdot \sigma \cdot p \cdot b \cdot \frac{I_{hm}}{N_p} \cdot S_p - \mu_p \cdot (N_p - S_p) + (m[t] \cdot R_p) \quad (1)$$

$$\frac{dI_p}{dt} = \alpha_1[t] \cdot \sigma \cdot p \cdot b \cdot \frac{I_h m}{N_p} \cdot S_p - (\gamma_p \cdot I_p) - (\mu_p \cdot I_p) - (\mu_{v1} \cdot I_p) \quad (2)$$

$$\frac{dR_p}{dt} = (\gamma_p \cdot I_p) \cdot (1 - \mu_{v1}) - (\mu_p \cdot R_p) - (m[t] \cdot R_p) \quad (3)$$

$$(4)$$

Marmosets

$$\frac{dS_c}{dt} = -\alpha_1[t] \cdot \sigma \cdot p \cdot b \cdot \frac{I_{hm}}{N_c} \cdot S_c - \mu_c \cdot (N_c - S_c) \quad (5)$$

$$\frac{dI_c}{dt} = \alpha_1[t] \cdot \sigma \cdot p \cdot b \cdot \frac{I_{hm}}{N_c} \cdot S_c - (\gamma_c \cdot I_c) - (\mu_c \cdot I_c) \quad (6)$$

$$\frac{dR_c}{dt} = (\gamma_c \cdot I_c) \cdot (1 - \mu_{v3}) - (\mu_c \cdot R_c) \quad (7)$$

Humans

$$\frac{dS_h}{dt} = -(\alpha_2[t] \cdot (1-p) \cdot b \cdot \frac{I_{hm}}{N_h}) \cdot S_h - (\alpha_a[t] \cdot b \cdot \frac{I_{aa}}{N_h} \cdot S_h - \mu_h \cdot (N_h - S_h) - (V[t] \cdot S_h) \quad (8)$$

$$\frac{dE_h}{dt} = (\alpha_2[t] \cdot (1-p) \cdot b \cdot \frac{I_{hm}}{N_h} \cdot p) \cdot S_h + \alpha_1[t] \cdot b \cdot \frac{I_{aa}}{N_h} \cdot S_h - (\delta_h \cdot E_h) - (\mu_h \cdot E_h) - (V[t] \cdot E_h) \quad (9)$$

$$\frac{dI_h}{dt} = (\delta_h \cdot E_h) - (\gamma_h \cdot I_h) - (\mu_h \cdot I_h) - (V[t] \cdot I_h) \quad (10)$$

$$\frac{dR_h}{dt} = (\gamma_h \cdot I_h) \cdot (1 - \mu_{v2}) - (\mu_h \cdot R_h) + (V[t] \cdot N_h) \quad (11)$$

$$(12)$$

***Haemagogus* mosquitoes**

$$\frac{dS_{hm}}{dt} = -((\alpha_1[t] \cdot \sigma \cdot p \cdot pMI_1 \cdot \frac{I_p}{N_p}) + (\alpha_2[t] \cdot (1-p) \cdot pMI_2 \cdot \frac{I_h}{N_h}) + \quad (13)$$

$$(\alpha_1[t] \cdot \sigma \cdot p \cdot pMI_4 \cdot \frac{I_c}{N_c})) \cdot S_{hm} + \mu_{hm} \cdot (N_{hm} - S_{hm}) \cdot N_{hm} \cdot (1 - \frac{N_{hm}}{K[t]} \quad (14)$$

$$\frac{dE_{hm}}{dt} = ((\alpha_1[t] \cdot \sigma \cdot p \cdot pMI_1 \cdot \frac{I_p}{N_p}) + (\alpha_2[t] \cdot (1-p) \cdot pMI_2 \cdot \frac{I_h}{N_h}) + \quad (15)$$

$$(\alpha_1[t] \cdot \sigma \cdot p \cdot pMI_4 \cdot \frac{I_c}{N_c})) \cdot S_{hm} - (PDR_{hm} + \mu_{hm}) \cdot E_{hm} \quad (16)$$

$$\frac{dI_{hm}}{dt} = (PDR_{hm} \cdot E_{hm}) - (\mu_{hm} \cdot I_{hm}) \quad (17)$$

(18)

***Aedes aegypti* mosquitoes**

$$\frac{dS_{aa}}{dt} = -(\alpha_1[t] \cdot pMI_3 \cdot \frac{I_h}{N_h}) \cdot S_{aa} \cdot \mu_{aa} \cdot (N_{aa} - S_{aa}) \cdot N_{aa} \cdot (1 - \frac{N_{aa}}{K[t]} \quad (19)$$

$$\frac{dE_{aa}}{dt} = (\alpha_1[t] \cdot pMI_3 \cdot \frac{I_h}{N_h}) \cdot S_{aa} - (PDR_{aa} + \mu_{aa}) \cdot E_{aa} \quad (20)$$

$$\frac{dI_{aa}}{dt} = (PDR_{aa} + E_{aa}) - (\mu_{aa} \cdot I_{aa}) \quad (21)$$

(22)

Carrying capacity

$$K[t] = \frac{K_{wet} + K_{dry}}{2} + \frac{K_{wet} - K_{dry}}{2} \cdot cos\frac{4t \cdot \pi}{days} \quad (23)$$

5.2 Simulations

To assess the role of rainfall seasonality in driving the YFV epidemic, we simulated disease transmission with four models with different seasonal drivers. The base model included seasonally-driven carrying capacity, mosquito biting rates, and howler monkey movement from the forest to the city. Carrying capacity is commonly treated as seasonal (e.g., [39]), whereas the pervasiveness and importance of seasonally driven biting rates and movement are less well understood. Thus, the three other models tested the importance of these factors in nested versions of the base model: model two included seasonally-driven monkey movement but not seasonally-driven mosquito biting; model three included seasonally-driven mosquito biting but not seasonally-driven monkey movement; and model four excluded both seasonally-driven monkey movement and mosquito biting.

Since some parameter values are less certain than others, we assessed the sensitivity of the model outcomes to the most uncertain parameter values. In the sensitivity analysis, we evaluated the impact of increasing and decreasing three highly uncertain parameters resulting in six model specifications. The six models used the base model but replaced the following parameter values: models 1-2) low/high YFV-induced monkey mortality rates; models 3-4) low/moderate proportion of *Haemogogus* mosquitoes biting non-human primates versus humans; and models 5-6) moderate/high movement rate of the monkeys to the city.

To assess the extent to which different interventions could have prevented the second wave of the YFV epidemic and beyond, we generated four model specifications representing 1) vector control (i.e., larvicide spraying in wet seasons); 2) conservation

Table 2 Model parameter symbols, definitions, and values. Numbers in brackets indicate low, moderate, and/or high estimates, which were used in the sensitivity analysis.

Parameter	Definition	Value
α_1	Biting rate of *Haemogogus* mosquitoes on primates	0.7 [0.5, 1.0]
α_2	Biting rate of *Haemogogus* mosquitoes on humans and *Aedes* mosquitoes on humans	0.35
σ	Percentage of *Haemogogus* bites on Howler monkeys (vs marmosets)	0.5
pMI_1	Probability of *Haemogogus* infection given a bite on infectious monkey	0.2
pMI_2	Probability of *Haemogogus* infection given a bite on infectious human	0.25
pMI_3	Probability of *Aedes* infection given a bite on infectious human	0.25
pMI_4	Probability of *Haemogogus* infection given a bite on infectious marmoset	0.125
b	Probability mosquito is infectious given infection	0.5
PDR_{hm}	YFV viral extrinsic incubation rate (i.e., development rate) in *Haemogogus*	0.083333
PDR_{aa}	YFV viral extrinsic incubation rate (i.e., development rate) in *Aedes*	0.076923
μ_{hm}	*Haemogogus* birth/mortality rate	0.05 [0.04, 0.14]
μ_{hm}	*Aedes* birth/mortality rate	0.05 [0.03, 0.10]
μ_p	Primate birth/mortality rate	0.000157
μ_h	Human birth/mortality rate	3.70E-05
μ_c	Marmoset birth/death rate	0.000457
μ_{v1}	Mortality rate of primates infected with YFV	0.5 [0.2, 0.8]
μ_{v2}	Mortality rate of humans infected with YFV	0.02
μ_{v3}	Mortality rate of marmosets infected with YFV	0.01
γ_p	Primate recovery rate (1/infectious period)	0.166667
γ_h	Human recovery rate (1/infectious period)	0.285714
γ_C	Marmoset recovery rate (1/infectious period)	0.25
δ_h	Human intrinsic incubation period	0.23
p	Probability *Haemogogus* biting a non-human primate (vs a human)	0.7 [0.3, 0.5]
m	Movement of Howler monkeys from the forest to the city (%/month)	0.5 [2, 10]
K_{dry}	Carrying capacity in dry season	300000
K_{wet}	Carrying capacity in wet season	1800000
V	Vaccination rate (per day)	0.00067

measures to reduce monkey movement into urban habitats; 3) earlier deployment of vaccines (three months earlier than actual deployment, corresponding with the initial outbreak, and continuing with early childhood vaccination campaigns); and 4) a combination of all three interventions. We ran the intervention simulations for eight years to assess whether interventions were effective in the short and long term.

For all 14 model specifications (four assessing the role of seasonality, six assessing parameter uncertainty, and four assessing interventions), we rain the simulations 500 times to account for initial condition uncertainty (i.e., compartment values at the start of the simulation period). We show the distributions for these starting values in appendix Table A1.

5.3 Data

We obtained monthly confirmed human and non-human primate cases from the Brazilian national health surveillance system, Sistema de Informação de Agravos de Notificação (SINAN). Human cases were confirmed as acute YFV based on serology or polymerase chain reaction (PCR). Non-human primates were tested for YFV by the Division of Zoonoses and Vector-borne Diseases. We used pooled cases of five genera

of non-human primates, predominately from the genus *Aloutta* (i.e., howler monkeys), but also composed of *Calithrix* (i.e., marmosets), Cebus, Saimiri, and Sapajus.

To contextualize the drought preceding the outbreak within historical and future climate conditions, we assessed two metrics of precipitation. We used the Standardized Precipitation Evapotranspiration Index (SPEI) based on weather station data to assess observed conditions between 2007 and 2020 in Minas Gerais, Brazil from [6]. The index measures water balance, with negative numbers indicating a water deficit. To assess how dry conditions may change in the future in this region, we visualized distributions of historical and future mean monthly evapotranspiration minus precipitation from six models participating in the Coupled Model Intercomparison Project Phase 6 (CMIP6) [40]: GFDL-CM4, GFDL-ESM4, CESM2-WACCM, CESM2, MPI-ESM1-2-HR, and MPI-ESM1-2-LR. For future projections, we used the SSP2-4.5 scenario, which represents a moderate pathway of greenhouse gas emissions. We estimated return periods by fitting a normal distribution to the precipitation data and using its parameters (mean and standard deviation) to calculate the value corresponding to an exceedance probability of 1/return period. This approach estimates the threshold value that corresponds to a specified frequency of exceedance. To compare the relative magnitude of two exceedance values (e.g., historical vs future 100-yr return period), we calculated the ratio of the larger exceedance value to the smaller one. This ratio quantifies how many times the larger value exceeds the smaller one, providing a sense of their relative difference in terms of magnitude or return period.

5.4 Validation

We evaluated how well each model specification (with the exception of the intervention scenarios) generated yellow fever virus transmission dynamics by correlating time series of model simulations with observational data. We calculated correlation between monthly predictions and observations using the cross-correlation function in base R. For the non-human primate comparison, we used no time lag, whereas for the human cases we used a one month lead time. We used a lead time for human cases because the observational data was aggregated to monthly case counts, but in reality, cases could have occurred up to 30 days apart. Anecdotally, the infected non-human primate carcasses were found prior to the peak in human cases suggesting a lag of a few weeks, despite the data showing peaks in the two populations in the same month each year. For each model specification, we calculated the correlation between observations (i.e., reported cases/deaths) and median model predictions for humans and non-human primates (howler monkeys only), adjusted based on expected reporting rates (0.7 for non-human primates because mortality rates are high and 0.12 for humans based on [19]). We determined the best fit model as the model that best characterized both human and non-human primate infection (i.e., highest average correlation across the two categories).

Acknowledgements

We acknowledge Wenchang Yang for guidance on using CMIP6 data.

Declarations

- Funding: JMC was supported by the Princeton University Climate and Disease programme with funding from the High Meadows Environmental Institute Grand Challenges and Environmental Studies Strategic Fund and the Joseph and Susan Gatto Foundation. JIR was supported by the National Institutes of Health (NIH K32AI168581).
- The authors declare no conflict of interest/competing interests.
- Data and code are available in the following github repository.
- Author contribution: JMC and JIR conceived of study and drafted the manuscript. All authors contributed intellectually to methodology, interpretation of results and figures, and manuscript edits.

Figures

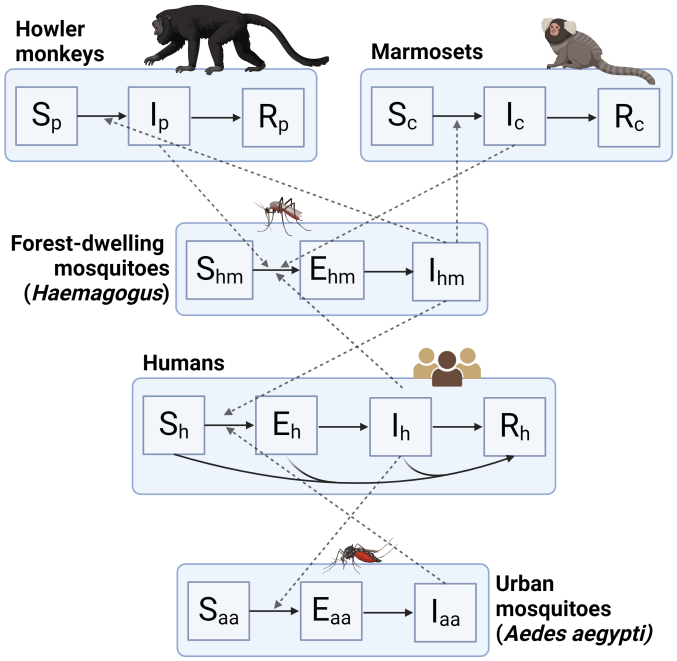

Fig. 1 Compartmental model of yellow fever virus transmission in Brazil. Each blue box indicates a different species involved in disease transmission. Individuals within each species can move sequentially through several health states: susceptible (S), exposed (E), infectious (I), and removed (R). Non-human primates do not include an exposed state because it is unknown whether they have a latent period and how long it would last. Mosquitoes do not have a removed state because their lifespan is short relative to the study period. Solid arrows indicate the direction individuals move between compartments and dashed arrows indicate the direction of transmission. The curved arrows in the human population represent vaccination.

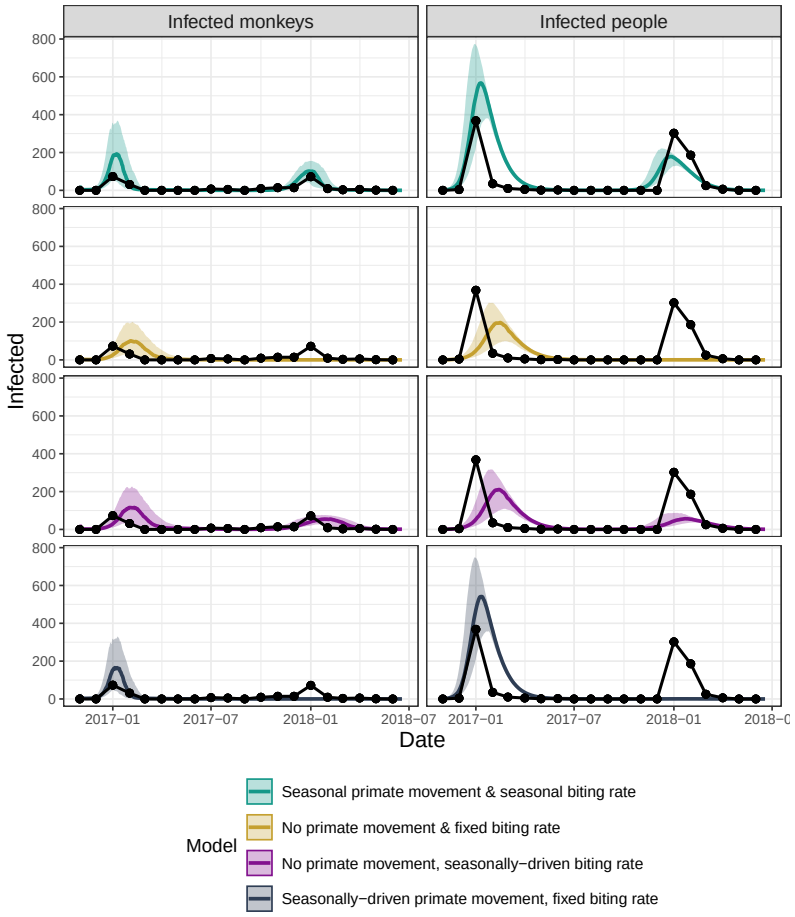

Fig. 2 Seasonally-driven non-human primate movement and mosquito biting contributed to driving the two-wave YFV epidemic in Brazil. Comparison of four nested models with observations for non-human primate cases (left) and human cases (right, lead time = one month). The base model (teal) included seasonally-driven primate movement and mosquito biting. The model with seasonally-driven mosquito biting (purple) holds primate movement constant and predicted late epidemic peaks. The model with seasonally-driven primate movement (dark blue) holds seasonally-driven mosquito biting constant and predicted no second wave. The model that holds both seasonally-driven primate movement and mosquito biting constant (orange) predicted a late first wave and no second wave of transmission. We show observations overlaid for comparison (black dots connected by lines).

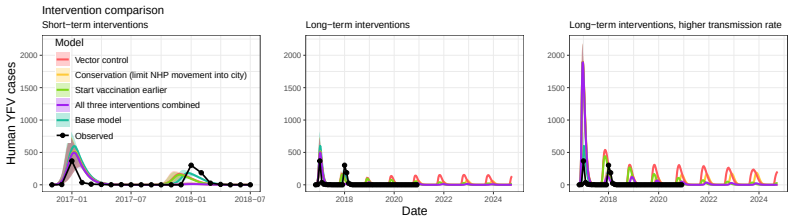

Fig. 3 Deploying multiple control strategies simultaneously are needed for sustained YFV control. Affects of interventions in the short-term (left) and long-term (right). We simulated four intervention strategies: vector control (i.e., reducing mosquito populations in the rainy season; pink), conservation initiatives (i.e., reducing primate movement into the cities; orange), early and continued vaccine distribution (green), and a combination of all three (dark blue). For comparison, we show observations (black points connected by lines) and the base model (teal).

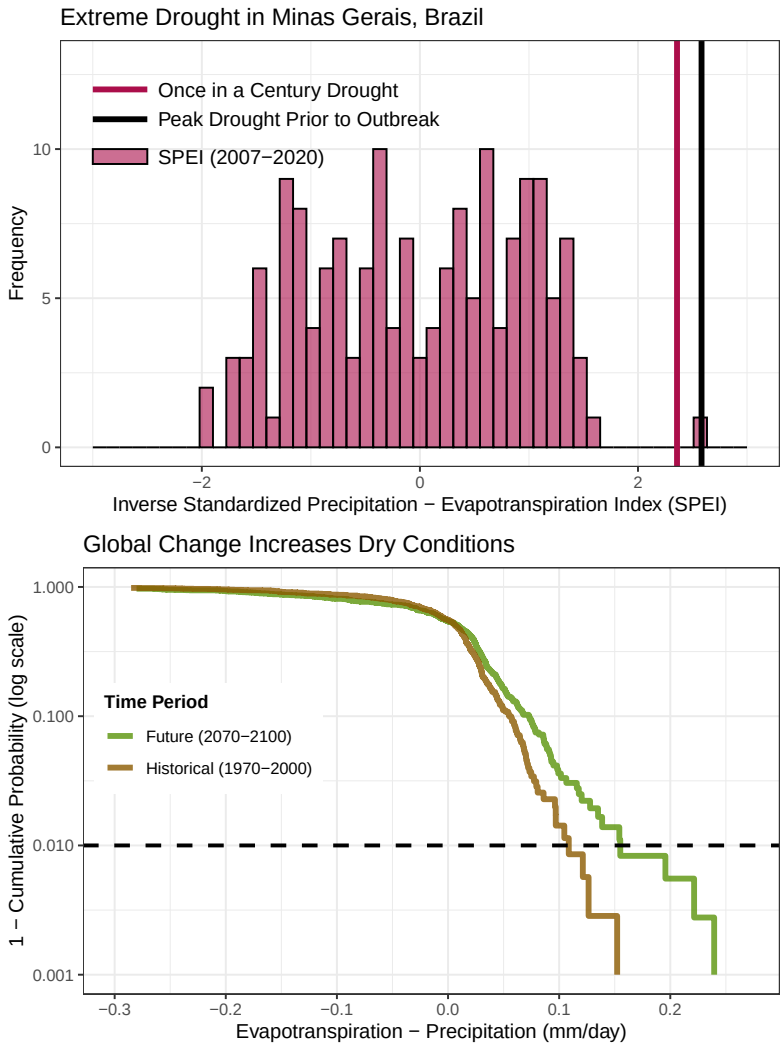

Fig. 4 Conditions preceding the YFV outbreak was more extreme than a once in a century drought and global change will give rise to more extreme dry conditions in the future. Histogram of the inverse Standardized Precipitation-Evapotranspiration Index (SPEI) for Minas Gerais, Brazil (top). We show the value for a once in a century drought (pink vertical line) and the value for SPEI preceding the YFV outbreak (black vertical line). A cumulative distribution function (CDF) plot (bottom) shows the survival probability (1 - CDF) of the difference between evapotranspiration and precipitation (mm/day) for two time periods: Historical (1970–2000) and Future (2070–2100). We plotted the y-axis in log space to highlight extreme events, with a dashed horizontal line indicating a 1% exceedance threshold. The plot illustrates an increased likelihood of extreme dry conditions in the future compared to the historical period. For top and bottom plots, negative number indicate wetter conditions and positive numbers indicate drier conditions.

Appendix A Sensitivity analysis

The model results were relatively robust to highly uncertain parameters (Appendix Figure A1, Appendix Table A2). Increasing or decreasing the YFV-induced monkey mortality rate changed the incidence slightly. Decreasing the proportion of *Haemogogus* mosquitoes biting NHP versus humans reduced the incidence in both NHP and humans. The model was most sensitive to changes in the movement rate of monkeys from the forest to the city. Increasing the movement rate increased incidence and caused an earlier second peak. The average correlation across all sensitivity analysis simulations was lower than the base model, however, certain specifications did improve the fit of the model predictions to human cases by increasing incidence during the second wave (the base model under-predicted the second wave). However, this improvement came at the cost of a considerable reduction in the fit between the model predictions and NHP cases, as well as decreasing the fit to human cases for the first wave and slightly offsetting the peak timing of the second wave.

Table A1 Distribution functions for generating the 500 initial condition values. Note that the *Haemogogus* mosquito and marmoset populations are proportions of the *Aedes aegypti* and howler monkey populations; thus, the initial conditions for these compartments varied across the simulations accordingly producing variation in initial conditions for five compartments.

Compartment	Distribution function
S_{aa}	˜Normal(300000, 100000)
S_p	˜Uniform(35000, 10000)
R_p	˜Normal(0.7, 0.1)

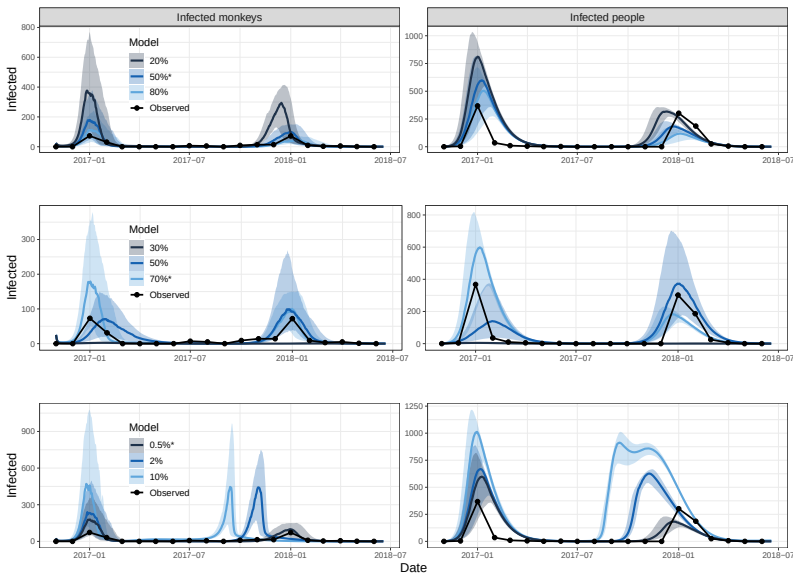

Fig. A1 Model results are relatively robust to uncertain parameter values. Infected monkeys (left) and infected people (right). Comparison of model simulations using low and high YFV-induced monkey mortality rates (top), low and moderate proportion *Haemogogus* mosquitoes biting non-human primates versus humans (middle) and moderate and high monkey movement rates (bottom). We indicated the values used in the base model with an asterisk and show observations (black points connected with lines) for comparison.

Table A2 Correlation between model predictions and observations across nested seasonally-driven models. Note that the 'No seasonality' model still includes a seasonal mosquito carrying capacity. We included the base model in the table for comparison.

Model	Human cases	NHP cases	Average correlation
Base model	0.16	0.93	0.55
Low YFV-monkey mortality rate	0.31	0.71	0.51
Moderate YFV-monkey mortality rate	0.07	0.86	0.47
Low prop. Hm biting NHP vs humans	0.32	-0.05	0.14
Moderate prop. Hm biting NHP vs humans	0.42	0.63	0.53
Moderate monkey movement rate	0.29	0.37	0.33
High monkey movement rate	0.23	0.61	0.42

References

[1] Silva, N. I. O. *et al.* Recent sylvatic yellow fever virus transmission in Brazil: the news from an old disease. *Virology Journal* **17**, 9 (2020). URL https://doi.org/10.1186/s12985-019-1277-7.

[2] Sacchetto, L. *et al.* Neighbor danger: Yellow fever virus epizootics in urban and urban-rural transition areas of Minas Gerais state, during 2017-2018 yellow fever outbreaks in Brazil. *PLoS neglected tropical diseases* **14**, e0008658 (2020).

[3] Chippaux, J.-P. & Chippaux, A. Yellow fever in Africa and the Americas: a historical and epidemiological perspective. *Journal of Venomous Animals and Toxins including Tropical Diseases* **24**, 20 (2018). URL https://doi.org/10.1186/s40409-018-0162-y.

[4] Vasconcelos, P. F. C. in *Yellow Fever* (ed.Marcondes, C. B.) *Arthropod Borne Diseases* 101–113 (Springer International Publishing, Cham, 2017). URL https://doi.org/10.1007/978-3-319-13884-8_8.

[5] Hill, S. C. *et al.* Climate and land-use shape the spread of zoonotic yellow fever virus. *medRxiv* (2022). URL https://www.medrxiv.org/content/early/2022/08/26/2022.08.25.22278983.

[6] Rosser, J. I., Nielsen-Saines, K., Saad, E. & Fuller, T. Reemergence of yellow fever virus in southeastern brazil, 2017–2018: What sparked the spread? *PLOS Neglected Tropical Diseases* **16**, 1–16 (2022). URL https://doi.org/10.1371/journal.pntd.0010133.

[7] Gómez, M. M. *et al.* Genomic and structural features of the yellow fever virus from the 2016-2017 Brazilian outbreak. *The Journal of General Virology* **99**, 536–548 (2018).

[8] Possas, C. *et al.* Yellow fever outbreak in Brazil: the puzzle of rapid viral spread and challenges for immunisation. *Memórias do Instituto Oswaldo Cruz* **113** (2018). URL https://www.ncbi.nlm.nih.gov/pmc/articles/PMC6135548/.

[9] Staples, J. E., Gershman, M., Fischer, M. & Centers for Disease Control and Prevention (CDC). Yellow fever vaccine: recommendations of the advisory committee on immunization practices (ACIP). *MMWR Recomm. Rep.* **59**, 1–27 (2010).

[10] Cunha, A. P. M. A. *et al.* Extreme Drought Events over Brazil from 2011 to 2019. *Atmosphere* **10**, 642 (2019). URL https://www.mdpi.com/2073-4433/10/11/642. Number: 11 Publisher: Multidisciplinary Digital Publishing Institute.

[11] Childs, M. L., Nova, N., Colvin, J. & Mordecai, E. A. Mosquito and primate ecology predict human risk of yellow fever virus spillover in Brazil. *Philosophical Transactions of the Royal Society B: Biological Sciences* **374**, 20180335 (2019).

URL https://royalsocietypublishing.org/doi/10.1098/rstb.2018.0335. Publisher: Royal Society.

[12] Chaves, L. F., Harrington, L. C., Keogh, C. L., Nguyen, A. M. & Kitron, U. D. Blood feeding patterns of mosquitoes: random or structured? *Frontiers in Zoology* **7**, 3 (2010). URL https://doi.org/10.1186/1742-9994-7-3.

[13] Amato, K. R. *et al.* Habitat degradation impacts black howler monkey (Alouatta pigra) gastrointestinal microbiomes. *The ISME Journal* **7**, 1344–1353 (2013). URL https://www.ncbi.nlm.nih.gov/pmc/articles/PMC3695285/.

[14] de Azevedo Fernandes, N. C. *et al.* Differential Yellow Fever Susceptibility in New World Nonhuman Primates, Comparison with Humans, and Implications for Surveillance. *Emerging Infectious Diseases* **27**, 47–56 (2021). URL https://www.ncbi.nlm.nih.gov/pmc/articles/PMC7774563/.

[15] Thoisy, B. d., Silva, N. I. O., Sacchetto, L., Trindade, G. d. S. & Drumond, B. P. Spatial epidemiology of yellow fever: Identification of determinants of the 2016-2018 epidemics and at-risk areas in Brazil. *PLOS Neglected Tropical Diseases* **14**, e0008691 (2020). URL https://journals.plos.org/plosntds/article?id=10.1371/journal.pntd.0008691. Publisher: Public Library of Science.

[16] Hindle, E. THE TRANSMISSION OF YELLOW FEVER. *The Lancet* **216**, 835–842 (1930). URL http://www.sciencedirect.com/science/article/pii/S0140673600897299.

[17] Estrada, A. & Coates-Estrada, R. Tropical rain forest fragmentation and wild populations of primates at Los Tuxtlas, Mexico. *International Journal of Primatology* **17**, 759–783 (1996). URL http://link.springer.com/10.1007/BF02735263.

[18] on Climate Change, I. P. *Climate Change Information for Regional Impact and for Risk Assessment*, 1767–1926 (Cambridge University Press, Cambridge, 2023).

[19] Johansson, M. A., Vasconcelos, P. F. C. & Staples, J. E. The whole iceberg: estimating the incidence of yellow fever virus infection from the number of severe cases. *Transactions of The Royal Society of Tropical Medicine and Hygiene* **108**, 482–487 (2014). URL https://doi.org/10.1093/trstmh/tru092.

[20] Couto-Lima, D. *et al.* Potential risk of re-emergence of urban transmission of Yellow Fever virus in Brazil facilitated by competent Aedes populations. *Scientific Reports* **7**, 4848 (2017). URL https://www.nature.com/articles/s41598-017-05186-3. Number: 1 Publisher: Nature Publishing Group.

[21] Lourenço-de Oliveira, R., Vazeille, M., Filippis, A. M. B. d. & Failloux, A.-B. Oral Susceptibility to Yellow Fever Virus of Aedes aegypti from Brazil. *Memórias do Instituto Oswaldo Cruz* **97**, 437–439 (2002). URL https://www.scielo.br/j/mioc/

a/krBLKYnBnGMVVBxgjZBCFzm/?lang=en. Publisher: Instituto Oswaldo Cruz, Ministério da Saúde.

[22] Abreu, F. V. S. d. *et al.* Haemagogus leucocelaenus and Haemagogus janthinomys are the primary vectors in the major yellow fever outbreak in Brazil, 2016-2018. *Emerging Microbes & Infections* **8**, 218–231 (2019).

[23] Cunha, M. S. *et al.* Possible non-sylvatic transmission of yellow fever between non-human primates in São Paulo city, Brazil, 2017–2018. *Scientific Reports* **10**, 15751 (2020). URL https://www.nature.com/articles/s41598-020-72794-x. Number: 1 Publisher: Nature Publishing Group.

[24] Cunha, M. S. *et al.* Epizootics due to Yellow Fever Virus in São Paulo State, Brazil: viral dissemination to new areas (2016–2017). *Scientific Reports* **9**, 5474 (2019). URL https://www.nature.com/articles/s41598-019-41950-3. Number: 1 Publisher: Nature Publishing Group.

[25] Pinheiro, G. G., Rocha, M. N., de Oliveira, M. A., Moreira, L. A. & Andrade Filho, J. D. Detection of Yellow Fever Virus in Sylvatic Mosquitoes during Disease Outbreaks of 2017–2018 in Minas Gerais State, Brazil. *Insects* **10**, 136 (2019). URL https://www.mdpi.com/2075-4450/10/5/136. Number: 5 Publisher: Multidisciplinary Digital Publishing Institute.

[26] Alencar, J. *et al.* Feeding Patterns of Haemagogus janthinomys (Diptera: Culicidae) in Different Regions of Brazil. *Journal of Medical Entomology* **42**, 981–985 (2005). URL https://doi.org/10.1093/jmedent/42.6.981.

[27] Alencar, J. *et al.* Distribution of Haemagogus and Sabethes Species in Relation to Forest Cover and Climatic Factors in the Chapada Dos Guimarães National Park, State of Mato Grosso, Brazil. *Journal of the American Mosquito Control Association* **34**, 85–92 (2018). URL https://meridian.allenpress.com/jamca/article/34/2/85/73692/Distribution-of-Haemagogus-and-Sabethes-Species-in. Publisher: Allen Press.

[28] Mucci, L. F. *et al.* Feeding habits of mosquitoes (Diptera: Culicidae) in an area of sylvatic transmission of yellow fever in the state of São Paulo, Brazil. *Journal of Venomous Animals and Toxins including Tropical Diseases* **21**, 1–10 (2015). URL https://www.scielo.br/j/jvatitd/a/QpyZbfn7wTZgTrSzT5FfYrC/?lang=en. Publisher: Centro de Estudos de Venenos e Animais Peçonhentos (CEVAP/UNESP).

[29] Liu, Y. & Rocklöv, J. What is the reproductive number of yellow fever? *Journal of Travel Medicine* **27**, taaa156 (2020). URL https://doi.org/10.1093/jtm/taaa156.

[30] Plowright, R. K. *et al.* Ecological countermeasures to prevent pathogen spillover and subsequent pandemics. *Nat. Commun.* **15**, 2577 (2024).

[31] Mueller, T. *et al.* How landscape dynamics link individual- to population-level movement patterns: a multispecies comparison of ungulate relocation data. *Global Ecology and Biogeography* **20**, 683–694 (2011). URL https://onlinelibrary.wiley.com/doi/abs/10.1111/j.1466-8238.2010.00638.x.

[32] Fortes, V. B., Bicca-Marques, J. C., Urbani, B., Fernández, V. A. & da Silva Pereira, T. in *Ranging behavior and spatial cognition of howler monkeys* (eds Kowalewski, M. M., Garber, P. A., Cortés-Ortiz, L., Urbani, B. & Youlatos, D.) *Howler Monkeys: Behavior, Ecology, and Conservation* 219–255 (Springer New York, New York, NY, 2015). URL https://doi.org/10.1007/978-1-4939-1960-4_9.

[33] Pozo-Montuy, G. & Serio-Silva, J. C. Movement and resource use by a group of alouatta pigra in a forest fragment in balancán, méxico. *Primates* **48**, 102–107 (2007).

[34] Santo, J. A. d. E. & Zocratto, K. B. F. Febre amarela: cobertura vacinal na região metropolitana de Belo Horizonte. *Revista Remecs - Revista Multidisciplinar de Estudos Científicos em Saúde* **4**, 26–34 (2019). URL https://www.revistaremecs.com.br/index.php/remecs/article/view/35. Number: 6.

[35] de Oliveira Figueiredo, P. *et al.* Re-Emergence of Yellow Fever in Brazil during 2016–2019: Challenges, Lessons Learned, and Perspectives. *Viruses* **12**, 1233 (2020). URL https://www.ncbi.nlm.nih.gov/pmc/articles/PMC7692154/.

[36] Amanna, I. J. & Slifka, M. K. Questions regarding the safety and duration of immunity following live yellow fever vaccination. *Expert Review of Vaccines* **15**, 1519–1533 (2016). URL https://doi.org/10.1080/14760584.2016.1198259. PMID: 27267203.

[37] Mukherjee, S., Mishra, A. & Trenberth, K. E. Climate change and drought: A perspective on drought indices. *Curr. Clim. Change Rep.* **4**, 145–163 (2018).

[38] Bicca-Marques, J. C. & de Freitas, D. S. The Role of Monkeys, Mosquitoes, and Humans in the Occurrence of a Yellow Fever Outbreak in a Fragmented Landscape in South Brazil: Protecting Howler Monkeys is a Matter of Public Health. *Tropical Conservation Science* **3**, 78–89 (2010). URL https://doi.org/10.1177/194008291000300107. Publisher: SAGE Publications Inc.

[39] Huber, J. H., Childs, M. L., Caldwell, J. M. & Mordecai, E. A. Seasonal temperature variation influences climate suitability for dengue, chikungunya, and zika transmission. *PLoS Negl. Trop. Dis.* **12**, e0006451 (2018).

[40] Eyring, V. *et al.* Overview of the coupled model intercomparison project phase 6 (cmip6) experimental design and organization. *Geoscientific Model Development* **9**, 1937–1958 (2016). URL https://gmd.copernicus.org/articles/9/1937/2016/.